JURNAL SAINS MATERI INDONESIA (JUSAMI)
ISSN: 1411-1098 (print), 2614-087X (online)
VOL. 26, ISSUE 1 2024
DOI: https://doi.org/10.55981/jsmi.2024.2051

ORIGINAL ARTICLE

Influence of Hydrothermal Temperature on the Physical Characteristics and Photocatalytics Activity of TiO_2 for Degradation of Amoxicillin

Sutisna[1*], R. R. Maulana[1], W. Maulina[1], Sujito[1], N. A. Berlianti[1] and E. Wibowo[2]

[1]Department of Physics, Faculty of Mathematics and Natural Sciences, Universitas Jember, East Java, Indonesia
[2]Engineering Physics, School of Electrical Engineering, Telkom University, Bandung, Indonesia

ABSTRACT – Titanium dioxide (TiO_2) is a photocatalyst material widely used for environmental remediation applications. In this research, TiO_2 material was synthesized using the hydrothermal method at various temperatures (150°C, 180°C, and 200°C). Based on the Fourier-transform infrared (FTIR) data, it was found that all the synthesized materials showed similar absorption peaks, and Ti-O-Ti bonds were detected, which is a characteristic of TiO_2. X-ray diffraction (XRD) analysis showed that all the synthesized materials were TiO_2 anatase with different crystalline sizes. The synthesized TiO_2 using the hydrothermal temperature of 180°C showed the smallest crystalline size of 86.81 nm. Based on the analysis of the band gap energy, it was found that wider band gap energy was obtained at higher hydrothermal temperatures. The band gap energies of the synthesized materials are 3.18 eV, 3.19 eV, and 3.21 eV for hydrothermal temperatures of 150°C, 180°C, and 200°C, respectively. The photocatalytic activity of the three synthesized materials was tested in the photodegradation experiment of amoxicillin under ultraviolet (UV) irradiation. As a result, it was found that TiO_2 synthesized at 180°C has the highest photocatalytic activity by degrading 100% of amoxicillin compounds within 120 minutes.

ARTICLE HISTORY
Received: 20 Oct 2023
Revised: 30 Mar 2024
Accepted: 02 Apr 2024

KEYWORDS
TiO_2
Photocatalytic activity
Hydrothermal
Hydrothermal temperature

INTRODUCTION

Titanium dioxide (TiO_2), also known as titania, is a transition metal oxide with the chemical formula TiO_2. Its application is very wide in many industrial applications such as paints, paper, plastics, inks, cosmetic products, and so on [1]–[3]. The TiO_2 material is unique in its optical, structural, electrical, and photocatalytic properties [4], [5]. In addition, TiO_2 is also chemically and physically stable, easy to synthesize, low-cost, non-toxic, has high reactivity, and has a high energy conversion efficiency [2], [6]. Based on these characteristics, TiO_2 is very suitable for other applications, such as solar cells [7], [8], fuel cells [4], [9], various sensors [10], wastewater treatment, self-cleaning layers [11], and disinfectants [12]. To date, TiO_2 nanomaterial is widely used in many applications, such as photocatalytic degradation of pollutants, antibacterial agents, supercapacitors, carbon dioxide (CO_2) reduction, sensors, solar cells, water separation, lithium-ion batteries, and many biomedical devices. [13]–[16]. TiO_2 has three crystal forms, namely anatase (tetragonal), rutile (tetragonal), and brookite (orthorhombic) [17]. This phase difference causes TiO_2 to have different properties and capabilities that affect its application. The anatase phase is widely used in photocatalysts because it has high photoactivity, while the rutile phase of TiO_2 is commonly used in pigment materials because it has high stability [18]. TiO_2 has energy band gaps of 3.20 eV, 3.02 eV, and 2.96 eV for the anatase, rutile, and brookite phases, respectively, and shows absorption in the ultraviolet (UV) region [2]. TiO_2's wide band gap and high rate of recombination of photoinduced charge carriers limit its potential applications in various fields. Therefore, band gap engineering is needed, which can be carried out using various methods such as optimization of synthesis parameters, doping, or coupling with other materials.

There are various methods for synthesizing TiO_2, such as sol-gel, electrochemical anodization, chemical vapor deposition, solvothermal, and hydrothermal methods [19]. Compared with other methods, hydrothermal is known as a simple and low-cost method, providing high purity and good dispersibility for synthesizing TiO_2 nanoparticles. [20]. The hydrothermal method refers to a heterogeneous reaction in the presence of a solvent under high-pressure conditions to crystallize a material that is relatively insoluble in water in a closed system [19]. This process is carried out in an autoclave, placed in an oven at a certain temperature. The advantages of the hydrothermal method are that the equipment used is simple, the reaction temperature is relatively low, it provides stoichiometric control, and it has good chemical homogeneity [21]. By using the hydrothermal method, it is very easy to control the shape and size of the synthesized material [19], [22]. Several other studies have also used the hydrothermal method to synthesize TiO_2-activated carbon composites to degrade methyl orange [23] and chromium [24]. Several results show that the TiO_2 crystallization process can be carried out without requiring a high-temperature calcination process. The hydrothermal method is carried out in a closed system to prevent the loss of solvent when heated so that the composition of the reactants during the synthesis process is not reduced. Heating water to a temperature near the boiling point will cause water vapor to form, which remains trapped in the system. The hydrothermal operational temperature during TiO_2 synthesis influences the

***CORRESPONDING AUTHOR** |sutisna | ✉ tissutisna@gmail.com

characteristics of the TiO_2 synthesized. This is because temperature can affect phase changes and the nucleation of a product [25]. Optimal temperature selection is needed to obtain TiO_2 with better photocatalytic characteristics and activity. By knowing the hydrothermal optimum temperature, energy use for the synthesis process also becomes more efficient. The use of TiO_2 materials in the environmental field gives satisfactory results. The TiO_2 photocatalyst can degrade organic pollutants into environmentally friendly compounds like CO_2 and H_2O. In this study, the photocatalytic activity of the synthesized TiO_2 material was evaluated in a photodegradation experiment of an antibiotic compound (amoxicillin). Not all antibiotics consumed by humans are absorbed by the body. About 30–90% of antibiotics are not absorbed by the body and are excreted into the environment through urine and feces. These unabsorbed antibiotics are mixed with water and cause environmental pollution [26]. Antibiotics mixed with water can disrupt the balance of the surrounding ecosystem. Antibiotics can also change the genetic nature of natural bacteria and make them resistant [27].

Based on the description above, this study aimed to determine the effect of hydrothermal operating temperature in the synthesis of TiO_2 on its physical characteristics and photocatalytic activity. The physical characteristics of the synthesized material were analyzed using the Fourier-transform infrared (FTIR) method, X-ray diffraction (XRD), and ultraviolet-visual (UV-Vis) spectrophotometry. The synthesized TiO_2 material is expected to be developed for general antibiotic waste treatment processes.

EXPERIMENTAL METHOD

Materials

The material which is used in the synthesis of titanium dioxide (TiO_2) was titanium tetraisopropoxide (TTIP) as a precursor (impurity 97%, Merck), and ethanol (assay range 99.8%(v/v), Merck). Meanwhile, the antibiotic used in the photodegradation test was amoxicillin trihydrate caplet 500 mg, produced by PT. Dankos Farma, with the molecular formula $C_{16}H_{19}N_3O_5$. The mass of one amoxicillin caplet is 670 mg, so the purity of the amoxicillin caplet is 74.6%.

Synthesis of TiO_2

Material synthesis was carried out using the hydrothermal method. The synthesis process was initiated by the preparation of a mixture consisting of 6 ml of TTIP, 35 ml of ethanol, and 35 ml of distilled water. This mixing process was carried out using a magnetic stirrer at a speed of 700 rpm for 1 hour. The resulting mixture was then put into the autoclave and heated in the oven. In this heating process, the hydrothermal process temperature was varied, namely 150°C, 180°C, and 200°C, for 12 hours. After this hydrothermal process, the samples were dried in an oven at a temperature of 100°C for 3 hours and calcined at a high temperature of 500°C for 3 hours. The calcination process is intended to increase the homogeneity of the TiO_2 crystals.

Materials Characterization

After the synthesis process, the next steps are material characterization and photocatalytic activity testing of the amoxicillin solution. The Fourier-transform infrared (FTIR) (Nicolet iS100, Thermo Scientific) was used to identify the molecular functional groups in the synthesized TiO_2 material. The X-ray diffraction (XRD) (D2 Phaser, Bruker) was used to evaluate the material's phase and crystallite size, and ultraviolet-visual diffuse reflectance spectroscopy (UV-Vis DRS) was used to assess the band gap energy of the synthesized TiO_2 material.

Photocatalytic Activity Test

A photodegradation experiment was used to examine the synthesized material's photocatalytic activity. A material dose of 0.5 g and a starting concentration of 22.39 ppm was employed in the 250 ml amoxicillin solution. The mass of one caplet of amoxicillin is 670 mg, so to make an amoxicillin solution with a concentration of 22.39 ppm, it needs 30 mg of amoxicillin caplets dissolved in one liter of distilled water. The photodegradation experiments were carried out in a UV chamber with three UV lamps (each at 10 watts) from the Evaco brand. During the photodegradation process, to disperse the TiO_2 material in the test solution while maximizing the UV irradiation process, the test solution was stirred using a magnetic stirrer at a speed of 350 rpm. Photodegradation experiments were carried out for 150 minutes, with solution sampling every 30 minutes to measure absorbance. Before absorbance measurements, the sample solution was centrifuged to separate TiO_2 from the test solution. The measurement of the absorbance of the test solution was carried out using a UV-Vis spectrophotometer. Based on the results of measuring the absorbance of the test solution, the degradation of amoxicillin can be determined.

RESULT AND DISCUSSION

Synthesized TiO_2 Materials

As explained in the materials and methods section, material synthesis is carried out using the hydrothermal method. Figure 1 shows the synthesized titanium dioxide (TiO_2) material with variations in hydrothermal operational temperature. The three materials produced are white and in powder form. The numbers 150, 180, and 200 in the samples' names refer to the operational hydrothermal temperature at which the TiO_2 sample was synthesized.

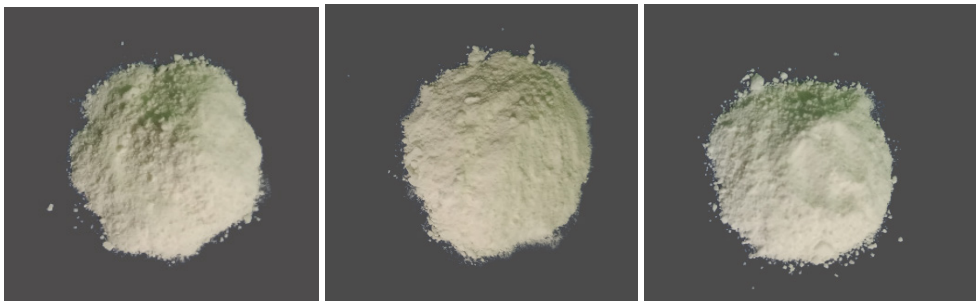

(a) (b) (c)

Figure 1. The synthesized TiO_2 material with variations in hydrothermal operational temperature: (a) TiO_2/150, (b) TiO_2/180, and (c) TiO_2/200

Characteristics of the Synthesized Material

Research in the field of nanomaterials cannot be separated from characterization activities. Material characterization aims to obtain information related to the specific properties of the material. The characterizations used in this study are Fourier-transform infrared (FTIR), X-ray diffraction (XRD), and ultraviolet-visual diffuse reflectance spectroscopy (UV-Vis DRS) spectrophotometers. FTIR characterization is carried out by knowing the infrared absorbance and transmittance spectra of the material. The absorption peaks of the infrared spectrum are specifically related to the functional groups in the material. The results of the FTIR characterization of the three synthesized TiO_2 materials with variations in hydrothermal operational temperature are shown in Figure 2.

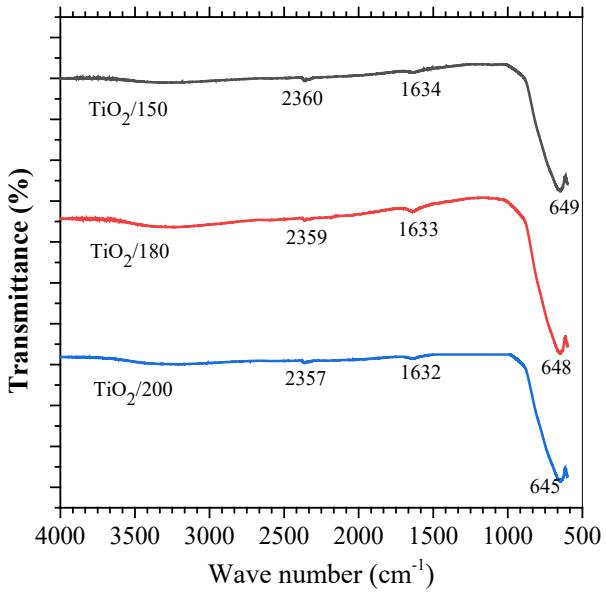

Figure 2. FTIR Spectra of Synthesized TiO_2

It can be seen from Figure 2 that the three variations of TiO_2 material produce relatively the same FTIR spectra. The spectra results show that there are three absorption peaks. The first absorption peaks in TiO_2/150, TiO_2/180, and TiO_2/200 materials are located at wave numbers 645 cm^{-1}, 648 cm^{-1}, and 649 cm^{-1}, respectively, which indicate the stretching vibration functional group of the Ti-O-Ti bond. The Ti-O-Ti functional group is the main functional group of TiO_2 [28]. The second absorption peaks in TiO_2/150, TiO_2/180, and TiO_2/200 materials are located at wave numbers 1632 cm^{-1}, 1633 cm^{-1}, and 1634 cm^{-1}, respectively, which indicates the presence of O-H hydroxyl groups. The presence of the -OH hydroxyl group is due to the presence of water compounds that are still left in the material or water vapor attached to the material during storage. Meanwhile, the third absorption peaks in TiO_2/150, TiO_2/180, and TiO_2/200 materials are located at wave numbers 2357 cm^{-1}, 2359 cm^{-1}, and 2360 cm^{-1}, respectively, indicating the presence of the C=O functional group. The C=O functional group is a material impurity that may be caused by ethanol during synthesis.

XRD characterization is used for crystal phase analysis by looking at the pattern of the peaks of the X-ray diffraction spectra of the material at a certain angle. The results of the XRD characterization of the three synthesized TiO_2 materials

with varying hydrothermal operating temperatures are shown in Figure 3. The XRD patterns of the three materials have relatively the same diffraction peaks. The source used as a reference is JCPDS Data No. 21-1272, which is the standard XRD pattern of anatase-phase TiO_2 material. The three materials have diffraction peaks almost the same as the peak pattern of the reference data. This shows that the three synthesized TiO_2 materials are in the anatase phase. Diffraction peaks can indicate crystal planes (hkl). The peaks of the diffraction angles are 25.281°, 37.601°, 48.050°, 53.891°, 55.046°, 62.690°, 68.762°, 70.311°, and 75.032°, which have planes (101), (004), (200), (105), (211), (204), (116), (220), and (215) as in Figure 3. Based on the XRD spectral data, the crystallite size of the material can be determined using the Deybe-Scherrer equation, as shown in equation (1):

$$D = \frac{K\lambda}{\beta cos\theta}. \quad (1)$$

The average crystallite size of each synthesized sample is shown in Figure 4. In Figure 4, the crystallite sizes of the materials are 86.806 nm, 93.483 nm, and 113.905 nm for TiO_2/180, TiO_2/200, and TiO_2/150, respectively. Based on these results, the difference in hydrothermal temperature affected the crystallite size of the synthesized TiO_2.

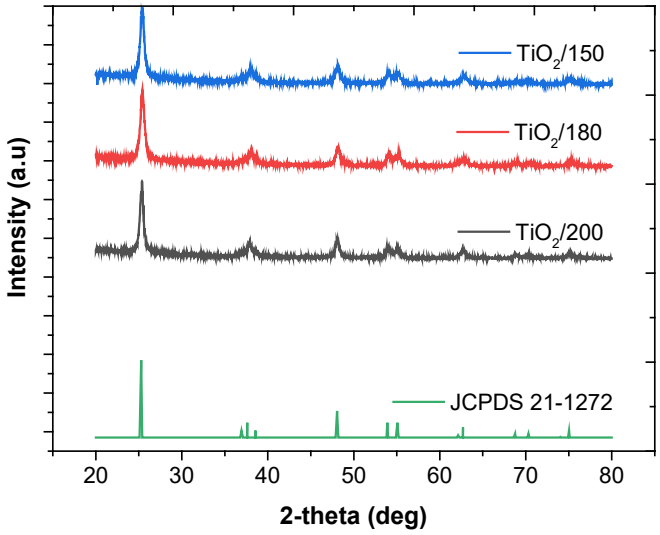

Figure 3. XRD spectra of the three synthesized TiO_2 materials

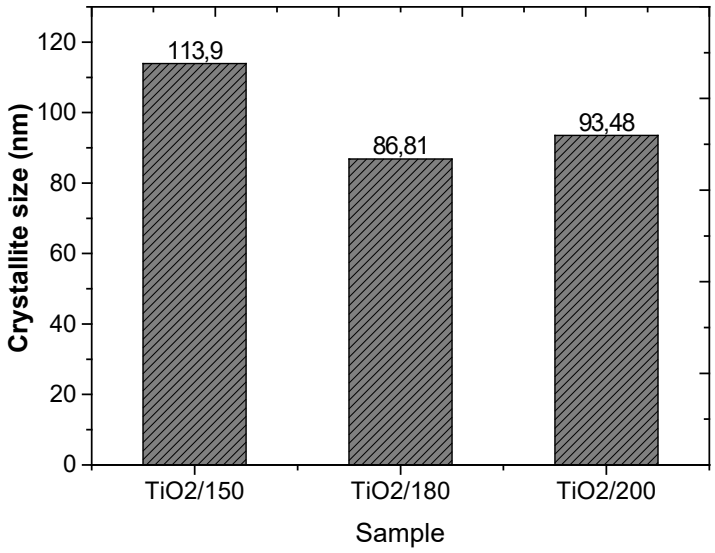

Figure 4. The crystallite size of the three synthesized TiO_2 materials

UV-Vis DRS characterization is carried out by irradiating ultraviolet until the visible light on the material, and then its reflection is analyzed. The UV-Vis DRS characterization results of the three synthesized TiO_2 materials with

variations in hydrothermal operational temperature are shown in Figure 5. The three synthesized TiO_2 variants show a relatively similar reflectance spectrum model. At a wavelength of 440–800 nm, the reflectance value is large and relatively constant, while at a wavelength of 440–363 nm, the reflectance value decreases significantly due to the transfer of electrons from the valence band to the conduction band. The reflectance value at a wavelength of 300–363 nm shows a small value and is relatively constant.

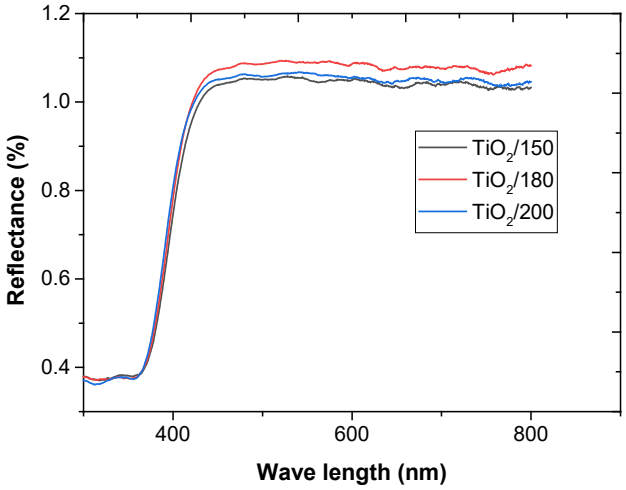

Figure 5. UV-Vis DRS characterization results of synthesized TiO_2

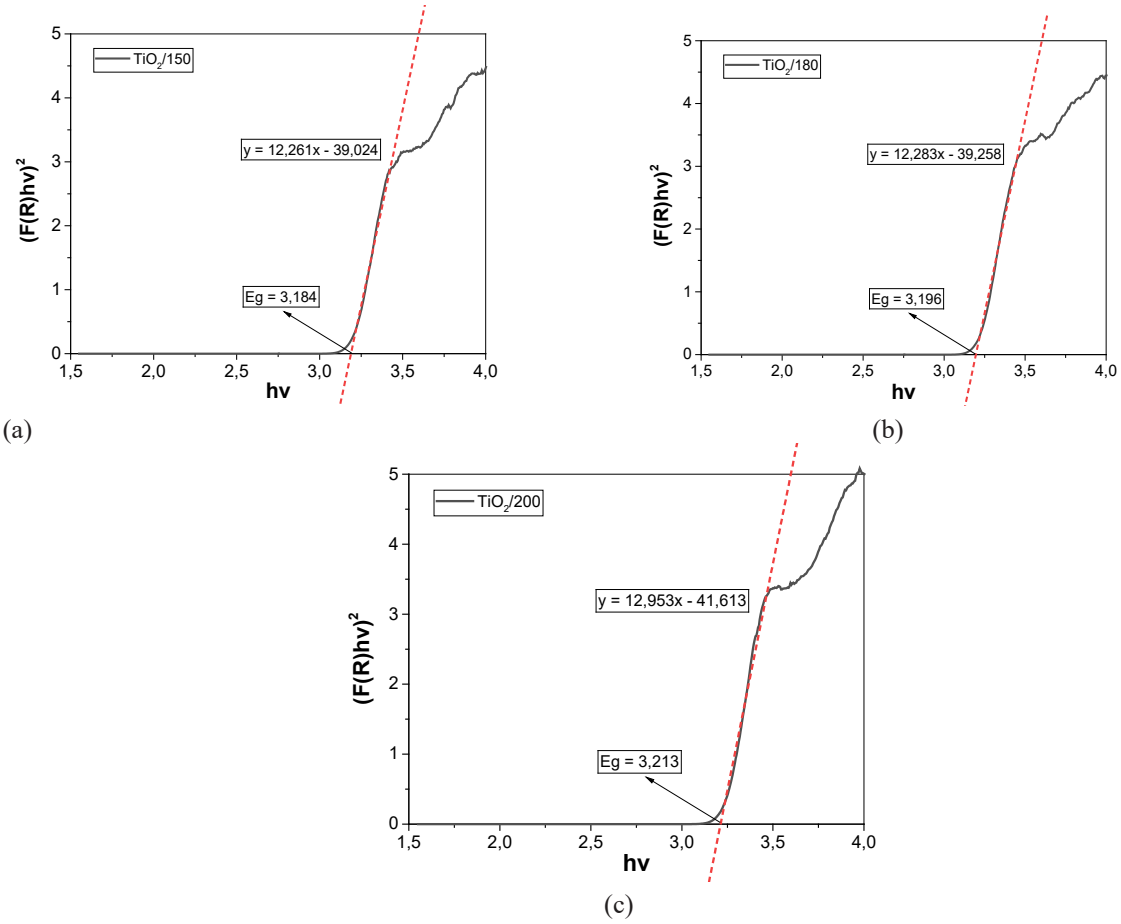

Figure 6. The bandgap energy of (a) TiO_2/150, (b) TiO_2/180, and (c) TiO_2/200

The band gap energy of the synthesized material can be analyzed using the Kubelka-Munk theory. The material absorption coefficient is proportional to the Kubelka-Munk factor $F(R)$, which satisfies the equation (2):

$$(R) = \frac{(1-R)^2}{(2R)}. \tag{2}$$

The relationship between the band gap energy and the absorption value is shown in equation (3):

$$(F(R)hv)^2 = A^2(hv - E_g)(F(R)hv)^2 = A^2(hv - E_g). \tag{3}$$

The band gap energy can be calculated by graphing the relationship between hv (photon energy) and $(F(R)hv)^2$ and drawing a linear line in the area with the steepest slope. The band gap energy value of the material is shown in Figure 6 as the energy value when $(F(R)hv)^2$ is null.

Figure 6 shows the results of the band gap energy analysis of the three synthesized materials. The three materials have nearly the same band gap energy. The band gap energies of TiO_2/150, TiO_2/180, and TiO_2/200 materials are 3.183 eV, 3.196 eV, and 3.213 eV, respectively. Based on these results, the greater the hydrothermal operational temperature, the wider the band gap energy value of the resulting material. The three synthesized TiO_2 materials have a very small band gap energy difference. This almost identical band gap energy occurs because the three materials are both in the anatase phase, which in the literature has a band gap energy of 3.2 eV [2]. The band gap energies of three variants of the synthesized TiO_2 from the literature are similar.

Photocatalytic Activity of Synthesized TiO_2

In this study, the photocatalytic activity of the synthesized TiO_2 material was tested in the photodegradation experiment of amoxicillin. The absorbance spectra during the photodegradation process of amoxicillin are shown in Figure 7. In Figure 7, the amoxicillin solution has the main absorbance peak at a wavelength of 227 nm. Figure 7 (a) is a graph of the absorbance of the test solution without adding TiO_2. The duration of UV irradiation has almost no effect on the absorbance of the amoxicillin solution. Meanwhile, the amoxicillin solution with the addition of TiO_2 experienced a change in the absorption peak that became increasingly sloping along with the duration of UV irradiation, as shown in Figure 7 (b), Figure 7 (c), and Figure 7 (d).

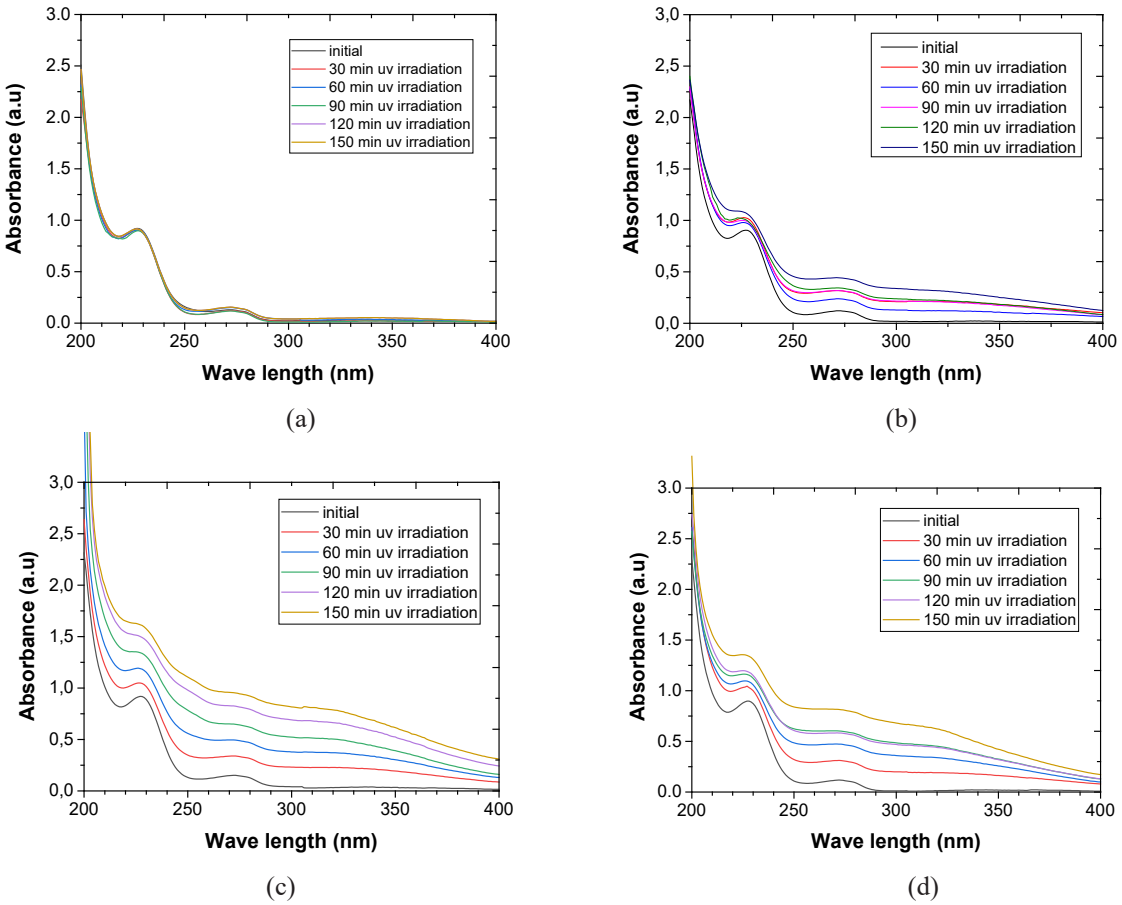

Figure 7. UV-Vis absorbance spectra of amoxicillin solution during photodegradation process (a) without TiO_2 (as an experiment control), (b) using TiO_2/150, (c) using TiO_2/180, and (d) using TiO_2/200.

The residual amoxicillin in the solution that has not been degraded (R%) is analyzed using the Lambert-Beer equation, which states that the peak absorbance is directly proportional to the concentration of the solution. To compare the concentrations of two or more solutions, the absorbance peak height (ΔA) can be used. The peak absorbance height (ΔA) is calculated by subtracting the peak absorbance value (A_{max}) from the valley absorbance value (A_{min}). A_{max} is located at a wavelength of 227 nm, while A_{min} is located at a wavelength of 219 nm, so R% is calculated by the equation (4):

$$R(\%) = \frac{\Delta A}{\Delta A_0}. \quad (4)$$

The R% graph generated from each sample as a function of irradiation time is shown in Figure 8.

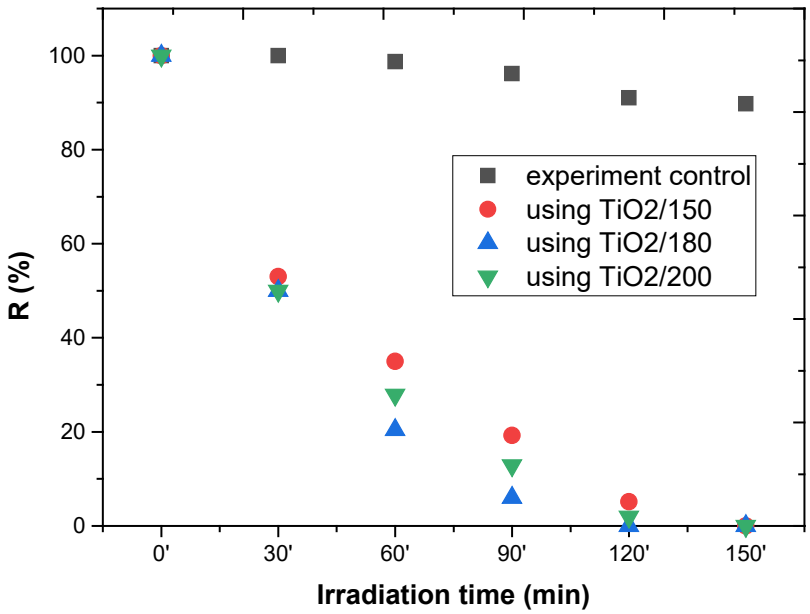

Figure 8. Graph of R% versus irradiation time

Based on Figure 8, the amoxicillin solution showed a decrease in concentration along with the duration of UV irradiation. Amoxicillin solution, which was not added with TiO_2 (only UV irradiated/photolysis), showed a decrease in concentration, although the rate was very low (10.26% for 150 minutes). On the other hand, for the material-treated amoxicillin solution, it appears that all the amoxicillin has been degraded during the 150 minutes of UV irradiation. The TiO_2/180 sample was able to degrade 100% of amoxicillin in 120 minutes, while at the same time, the TiO_2/150 and TiO_2/200 samples were able to degrade 94.87% and 98.02% of amoxicillin, respectively. In the degradation process, the amoxicillin compound with the molecular formula $C_{16}H_{19}N_3O_5$ decomposes into simpler compounds, namely CO_2, H_2O, and HNO_3 [29]. The graph of R% against time for three variations of TiO_2 satisfies an exponential equation, which can explain the reaction rate kinetics. The Langmuir-Hinshelwood equation of order 1 (L-H order 1) is shown in equation (5):

$$C/C_o = exp(-kt)C/C_o = exp(-kt). \quad (5)$$

Equation (3) can be used to describe the kinetics of photocatalytic reactions in general. In this equation, C is the concentration of the solution at a certain time, C_o is the concentration of the initial solution, k is the rate constant of the photocatalytic reaction, and t is the time. Figure 9 depicts the results of the first-order of L-H model fitting.

The data fitting has a fairly good approximation with R^2 values of 0.989, 0.993, and 0.995 for TiO_2/150, TiO_2/180, and TiO_2/200, respectively. From the fitting chart, it can be determined that the reaction rate constant (k) is 0.0198 min^{-1} for TiO_2/150, 0.0262 min^{-1} for TiO_2/180, and 0.0231 min^{-1} for TiO_2/200. These three kinetic rate constants are still greater

than those obtained by Wahyuni et al., which used Cr-doped TiO_2 to degrade amoxicillin residues. In their experiments, the photodegradation of amoxicillin using TiO_2-0.33Cr follows the pseudo-first-order kinetic model with a reaction rate constant (k) of 0.004 min^{-1} [30]. The value of the reaction rate constant describes how fast the photocatalytic process occurs. In this case, TiO_2/180 has the highest reaction rate of 0.0262 min^{-1}. This means that the TiO_2/180 material is able to reduce the C/C_o value by 0.0262 in one minute. Based on the research results that have been obtained, it show that the photocatalytic activity in each material is caused by the influence of hydrothermal operational temperature variations. Variations in the hydrothermal process temperature affect the crystalline size of the synthesized material, which in turn also affects the photocatalytic activity of the synthesized material. TiO_2/180 has the highest photocatalytic activity because it has the smallest crystal size, followed by TiO_2/200 and TiO_2/150 materials. The smaller the crystal size, the higher the photocatalytic activity. This happens because the smaller the crystal size of the material, the greater the surface area that reacts directly with pollutants, so the process of photocatalytic reactions occurs faster.

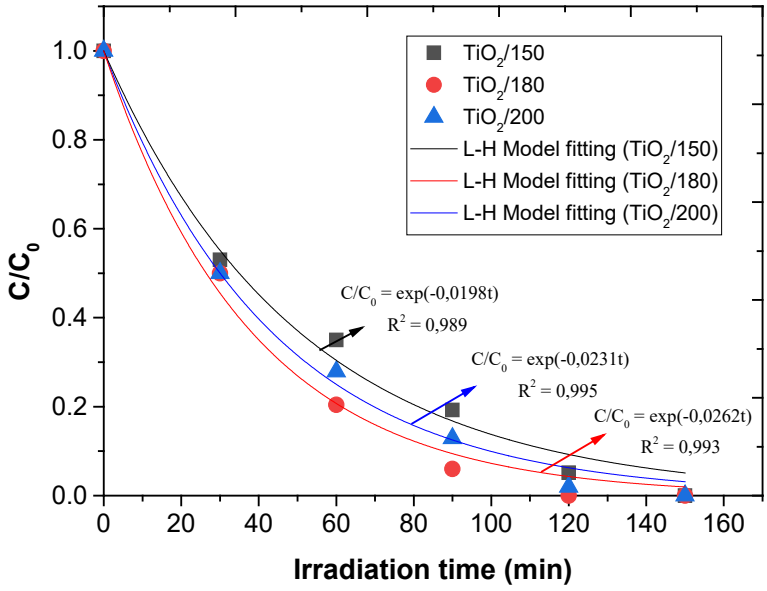

Figure 9. Results of first-order LH model fitting for photodegradation of amoxicillin with various treatments

CONCLUSION

From the research conducted, it can be concluded that variations in hydrothermal process temperatures (150°C, 180°C, and 200°C) affect several physical characteristics and the photocatalytic activity of the synthesized Titanium dioxide (TiO_2). The Fourier-transform infrared (FTIR) results show that the synthesized materials have relatively the same absorption peaks, with the presence of Ti-O-Ti bonds, which is a characteristic of TiO_2 material. X-ray diffraction (XRD) analysis shows that the synthesized material is anatase TiO_2 with different crystal sizes. TiO_2, which was synthesized at an operational temperature of 180°C, has the smallest crystal size of 86.81 nm. Based on the band gap energy analysis, it shows that the higher the synthesis temperature during the hydrothermal process, the wider the band gap energy of the synthesized TiO_2. The band gap energies of the synthesized materials are 3.18 eV, 3.19 eV, and 3.21 eV for TiO_2/150, TiO_2/180, and TiO_2/200, respectively. The photocatalytic activity of the three synthesized TiO_2 materials was tested in the photodegradation experiment of amoxicillin under ultraviolet (UV) irradiation. The results showed that TiO_2 synthesized at 180°C had the highest photocatalytic activity, degrading 100% of amoxicillin within 120 minutes.

ACKNOWLEDGEMENT

The authors thank the Universitas Jember for the financial support in this research through Hibah Reworking Skripsi/Tesis (Grant No. 6398/UN25.3.1/LT/2022).

REFERENCES

[1] S. Karim, P. Pardoyo, and A. Subagio. "Sintesis dan Karakterisasi TiO_2 Terdoping Nitrogen (N-Doped TiO_2) dengan Metode Sol–Gel." *Jurnal Kimia Sains dan Aplikasi*, vol. 19, no. 2, pp. 63–67, Aug. 2016.

[2] J. Prakash, S. Sun, H. C. Swart, and R. K. Gupta. "Noble Metals-TiO_2 Nanocomposites: From Fundamental Mechanisms to Photocatalysis, Surface Enhanced Raman Scattering and Antibacterial Applications." *Applied Materials Today*, vol. 11, pp. 82–135, Jun. 2018.

[3] A. J. Haider, Z. N. Jameel, and I. H. M. Al-Hussaini. "Review on: Titanium Dioxide Applications." *Energy Procedia*, vol. 157, pp. 17–29, Jan. 2019.

[4] J. Wang, S. Chen, D. Liu, C. Chen, R. Li, and T. Peng. "Fabrication of PbS Nanocrystal-Sensitized Ultrafine TiO_2 Nanotubes for Efficient and Unusual Broadband-Light-Driven Hydrogen Production." *Materials Today Chemistry*, vol. 17, p. 100310, Sept. 2020.

[5] T. N. Ravishankar, M. de O. Vaz, T. Ramakrishnappa, S. R. Teixeira, and J. Dupont. "Ionic Liquid–Assisted Hydrothermal Synthesis of Nb/TiO_2 Nanocomposites for Efficient Photocatalytic Hydrogen Production and Photodecolorization of Rhodamine B Under UV-Visible and Visible Light Illuminations." *Materials Today Chemistry*, vol. 12, pp. 373–385, Jun. 2019.

[6] B. Niu, X. Wang, K. Wu, X. He, and R. Zhang. "Mesoporous Titanium Dioxide: Synthesis and Applications in Photocatalysis, Energy and Biology." *Materials (Basel)*, vol. 11, no. 10, Oct. 2018.

[7] T. Buapuean and S. Jarudilokkul. "Synthesis of Mesoporous TiO_2 with Colloidal Gas Aphrons, Colloidal Liquid Aphrons, and Colloidal Emulsion Aphrons for Dye-Sensitized Solar Cells." *Materials Today Chemistry*, vol. 16, p. 100235, Jun. 2020.

[8] A. Singh, R. Ranjan, A. Garg, and R. Gupta, "Progress in tailoring perovskite based solar cells through compositional engineering: Materials properties, photovoltaic performance and critical issues," *Mater. Today Energy*, vol. 9, pp. 440–487, Aug. 2018, doi: 10.1016/j.mtener.2018.07.003.

[8] J. Prakash, A. Singh, G. Sathiyan, R. Ranjan, A. Singh, A. Garg, and R. K. Gupta. "Progress in Tailoring Perovskite Based Solar Cells through Compositional Engineering: Materials Properties, Photovoltaic Performance, and Critical Issues." *Materials Today Energy*, vol. 9, pp. 440–487, Sep. 2018.

[9] W. Dong, Y. Tong, B. Zhu, H. Xiao, L. Wei, C. Huang, B. Wang, X. Wang, J.-S. Kim, and H. Wang. "Semiconductor TiO_2 Thin Film as an Electrolyte for Fuel Cells." *Journal of Materials Chemistry A*, vol. 7, no. 28, pp. 16728–16734, Jul. 2019.

[10] S. T Thannickal, M. G. Gigimol, and B. Mathew. "A Brief Overview of Molecularly Imprinted Polymers Supported on Titanium Dioxide Matrices." *Materials Today Chemistry*, vol. 11, pp. 283–295, Mar. 2019.

[11] Y. Ren, W. Li, Z. Cao, Y. Jiao, J. Xu, P. Liu, S. Li, and X. Li. "Robust TiO_2 Nanorods-SiO_2 Core-Shell Coating with High-Performance Self-Cleaning Properties Under Visible Light." *Applied Surface Science*, vol. 509, p. 145377, Apr. 2020.

[12] S. Veziroglu, J. Hwang, J. Drewes, I. Barg, J. Shondo, T. Strunskus, O. Polonskyi, F. Faupel, and O. C. Aktas. "PdO Nanoparticles Decorated TiO_2 Film with Enhanced Photocatalytic and Self-Cleaning Properties." *Materials Today Chemistry*, vol. 16, p. 100251, Jun. 2020.

[13] K. K. Paul and P. K. Giri. "Shape Tailored TiO_2 Nanostructures and Their Hybrids for Advanced Energy and Environmental Applications: A Review." *Journal of Nanoscience and Nanotechnology.*, vol. 19, pp. 307–331, Jan. 2019.

[14] F. Xu, B. Zhu, B. Cheng, J. Yu, and J. Xu. "1D/2D TiO_2/MoS_2 Hybrid Nanostructures for Enhanced Photocatalytic CO_2 Reduction." *Advanced Optical Materials*, vol. 6, no. 23, p. 1800911, Oct. 2018.

[15] J. V. Patil, S. S. Mali, J. S. Shaikh, C. K. Hong, and P. S. Patil. "Electrochemically Anodized Ultralong TiO_2 Nanotubes for Supercapacitors." *Journal of Electronic Materials*, vol. 48, no. 2, pp. 873–878, Nov. 2019.

[16] Z. Chen, G. Zhang, J. Prakash, Y. Zheng, and S. Sun. "Rational Design of Novel Catalysts with Atomic Layer Deposition for the Reduction of Carbon Dioxide." *Advanced Energy Materials*, vol. 9, no. 37, p. 1900889, Aug. 2019.

[17] R. Verma, J. Gangwar, and A. K. Srivastava. "Multiphase TiO_2 Nanostructures: A Review of Efficient Synthesis, Growth Mechanism, Probing Capabilities, and Applications in Bio-Safety and Health." *RSC Advances*, vol. 7, no. 70, pp. 44199–44224, Sept. 2017.

[18] A. Fahmi, C. Minot, B. Silvi, and M. Causá. "Theoretical Analysis of the Structures of Titanium Dioxide Crystals." *Physical Review B*, vol. 47, no. 18, pp. 11717–11724, May 1993.

[19] R. Katal, S. Masudy-Panah, M. Tanhaei, M. H. D. A. Farahani, and H. Jiangyong. "A Review on the Synthesis of the Various Types of Anatase TiO_2 Facets and Their Applications for Photocatalysis." *Chemical Engineering Journal*, vol. 384, p. 123384, Mar. 2020.

[20] J. Cabrera, H. Alarcón, A. López, R. Candal, D. Acosta, and J. Rodriguez. "Synthesis, Characterization and Photocatalytic Activity of 1D TiO_2 Nanostructures." *Water Science and Technology*, vol. 70, no. 6, pp. 972–979, Jul. 2014.

[21] R. Hidayat, G. Fadillah, and S. Wahyuningsih. "A Control of TiO_2 Nanostructures by Hydrothermal Condition and Their Application: A Short Review." *IOP Conference Series Materials Science and Engineering*, vol. 578, p. 012031, Sept. 2019.

[22] A. H. Mamaghani, F. Haghighat, and C.-S. Lee. "Hydrothermal/Solvothermal Synthesis and Treatment of TiO_2 for Photocatalytic Degradation of Air Pollutants: Preparation, Characterization, Properties, and Performance." *Chemosphere*, vol. 219, pp. 804–825, Mar. 2019.

[23] S. Bagheri, Z. A. Mohd Hir, A. Termeh Yousefi, and S. B. Abd Hamid. "Photocatalytic Performance of Activated Carbon-Supported Mesoporous Titanium Dioxide." *Desalination and Water Treatment*, vol. 57, no. 23, pp. 10859–10865, 2016.

[24] D. Murtasima, Sutisna, B. E. Cahyono, E. Wibowo, and M. Rokhmat. "Synthesis of TiO_2 - Activated Carbon Composite (Variation of Activated Carbon Particles Size) and Its Photocatalytic Tests." *AIP Conference Proceedings*, vol. 2663, p. 50005, Sep. 2022.

[25] H. Hayashi and Y. Hakuta. "Hydrothermal Synthesis of Metal Oxide Nanoparticles in Supercritical Water." *Materials (Basel, Switzerland)*, vol. 3, no. 7, pp. 3794–3817, Jun. 2010.

[26] X. Hu, Q. Zhou, and Y. Luo. "Occurrence and Source Analysis of Typical Veterinary Antibiotics in Manure, Soil, Vegetables and Groundwater from Organic Vegetable Bases, Northern China." *Environmental Pollution*, vol. 158, no. 9, pp. 2992–2998, Sept. 2010.

[27] C. Tixier, H. P. Singer, S. Oellers, and S. R. Müller. "Occurrence and Fate of Carbamazepine, Clofibric Acid, Diclofenac, Ibuprofen, Ketoprofen, and Naproxen in Surface Water.," *Environmental Science & Technology*, vol. 37, no. 6, pp. 1061–1068, Feb. 2003.

[28] Maulidiyah, D. Wibowo, Hikmawati, R. Salamba, and M. Nurdin. "Preparation and Characterization of Activated Carbon from Coconut Shell-Doped TiO_2 in Water Medium." *Oriental Journal of Chemistry*, vol. 31, no. 4, pp. 2337–2342, 2015.

[29] E. T. Wahyuni, P. Y. Yulikayani, and N. H. Aprilita. "Enhancement of Visible-Light Photocatalytic Activity of Cu-Doped TiO_2 for Photodegradation of Amoxicillin in Water." *Journal of Materials and Environmental Science*, vol. 2020, no. 4, p. 670, 2020.

[30] E. T. Wahyuni, R. N. Cahyono, M. Nora, E. Z. Alharissa, and E. S. Kunarti. " Degradation of Amoxicillin Residue under Visible Light over TiO_2 Doped with Cr Prepared from Tannery Wastewater." *Results in Chemistry*, vol. 7, p. 101302, Jan. 2024.